Molecular Cell
Article

Robust Control of Nitrogen Assimilation by a Bifunctional Enzyme in *E. coli*

Yuval Hart,[1,3] Daniel Madar,[1,3] Jie Yuan,[2,3] Anat Bren,[1] Avraham E. Mayo,[1] Joshua D. Rabinowitz,[2] and Uri Alon[1,*]
[1]Department of Molecular Cell Biology, Weizmann Institute of Science, Rehovot 76100, Israel
[2]Lewis-Singer Institute for Integrative Genomics, Princeton University, Princeton, NJ 08544, USA
[3]These authors contributed equally to this work
*Correspondence: urialon@weizmann.ac.il
DOI 10.1016/j.molcel.2010.12.023

SUMMARY

Bacteria regulate the assimilation of multiple nutrients to enable growth. How is balanced utilization achieved, despite fluctuations in the concentrations of the enzymes that make up the regulatory circuitry? Here we address this question by studying the nitrogen system of *E. coli*. A mechanism based on the avidity of a bifunctional enzyme, adenylyltransferase (AT/AR), to its multimeric substrate, glutamine synthetase, is proposed to maintain a robust ratio between two key metabolites, glutamine and α-ketoglutarate. This ratio is predicted to be insensitive to variations in protein levels of the core circuit and to the rate of nitrogen utilization. We find using mass spectrometry that the metabolite ratio is robust to variations in protein levels and that this robustness depends on the bifunctional enzyme. Moreover, robustness carries through to the bacteria growth rate. Interrupting avidity by adding a monofunctional AT/AR mutant to the native system abolishes robustness, as predicted by the proposed mechanism.

INTRODUCTION

Cells take up multiple nutrients in order to grow and function. How can cells balance the uptake of different nutrients, so that appropriate ratios are achieved? Such balancing depends on biochemical regulatory circuits, which are made of proteins whose numbers fluctuate over time and from cell to cell. Furthermore, sources of nutrients can fluctuate over time. How can regulatory circuits cope with these uncertainties, to provide balanced nutrient uptake?

To address these questions, we study one of the best-characterized metabolic regulatory circuits, in the *E. coli* nitrogen assimilation system. This system takes up nitrogen in the form of ammonia to synthesize the amino acids glutamate and glutamine (Figure 1A). These two amino acids are the nitrogen donors for virtually all reactions requiring nitrogen in the cell (Neidhardt and Curtiss, 1996).

The key enzyme in this system, glutamine synthetase (GS), produces glutamine from glutamate and ammonia. GS has an elaborate control mechanism with several distinctive biochemical features. First, GS is a dodecamer made of 12 identical monomers. The activity of GS is determined by a reversible covalent modification: each monomer can be either adenylated or unadenylated, with adenylation inactivating the monomer's activity. The total activity of GS is the sum of its active monomers, without discernable cooperative effects (Shapiro and Stadtman, 1970; Rhee et al., 1989).

A second feature of this system is that the modification of GS is carried out by a bifunctional enzyme that catalyzes two opposing reactions. This enzyme, called adenylyltransferase/adenylyl-removing enzyme, AT/AR, both adds and removes the adenyl modification of GS, using two distinct domains (Jaggi et al., 1997). The rates of these opposing reactions depend on two inputs: glutamine and the TCA cycle metabolite α-ketoglutarate, which is the carbon backbone for glutamate and glutamine (Jiang et al., 2007a, 2007b). These inputs act both directly on AT/AR and through a regulatory protein called PII that binds AT/AR (Kamberov et al., 1995; Ninfa and Atkinson, 2000).

By responding to both glutamine and its carbon backbone, α-ketoglutarate, the nitrogen system effectively senses the ratio between nitrogen and carbon: nitrogen is represented by glutamine and carbon by α-ketoglutarate. Nitrogen shortage is reflected by reduced levels of glutamine and increased levels of α-ketoglutarate (Yuan et al., 2009; Brauer et al., 2006; Ikeda et al., 1996). While the ratio of glutamine to α-ketoglutarate varies dramatically in response to nitrogen limitation, this ratio is remarkably constant under other conditions, such as carbon limitation (Senior, 1975; Figure 1B). Such a constant ratio requires tuning the rate of ammonia assimilation to match precisely the carbon uptake rate, to avoid draining the carbon pool of the cell by producing too much glutamine—because synthesis of each glutamine molecule draws out one α-ketoglutarate molecule from the TCA cycle (Figure 1A).

The final step in the control of this system is transcriptional: when nitrogen limits growth, there is an increase in the transcription of the GS gene, controlled by the activator NtrC (Jiang et al., 1998).

Here we use theory and experiments to ask whether the unusual biochemical details of the nitrogen system have a functional meaning. Specifically, why does this system use a bifunctional enzyme that catalyzes two opposing reactions, and why is GS multimeric? Previous studies suggested a selective advantage for the bifunctional nature of AT/AR, such as to set the glutamine response point of the system (Stadtman and Chock, 1977).

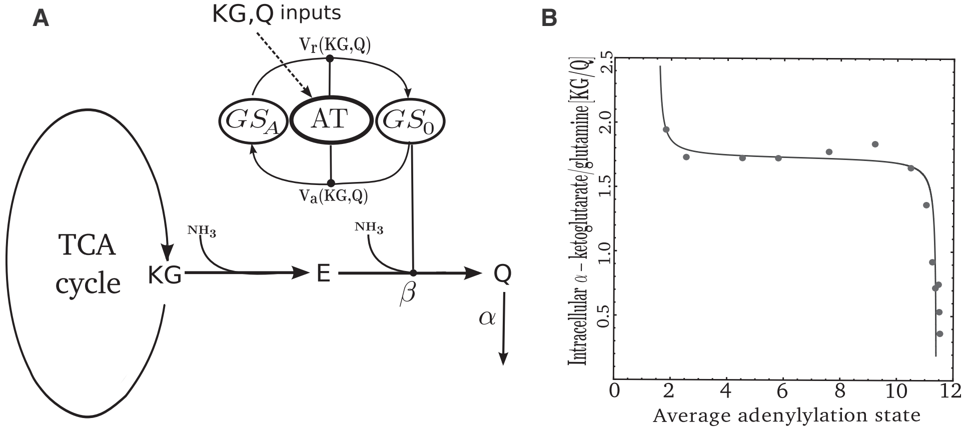

Figure 1. Glutamine Synthetase and Its Regulation in *E. coli*

(A) GS uses ammonia to produce glutamine (Q) from glutamate (E). It is active in its unadenylated form (GSo) and inactive when adenylated (GS_A). Adenyl modification is both added and removed by the bifunctional enzyme AT/AR (abbreviated here as AT). This enzyme is regulated by two input effectors, glutamine (Q) and α-ketoglutarate (KG). The latter is a TCA cycle intermediate and is the source for the carbon backbone of glutamate and glutamine.

(B) Shown are data from Senior (Senior, 1975) on the KG/Q ratio as a function of GS adenylation state during carbon limitation. Manipulation of carbon availability in a chemostat alters both the GS adenylation state and the KG/Q ratio, with increasing carbon availability associated with a lower GS adenylation (to increase nitrogen assimilation to keep up with carbon assimilation). Note that the KG/Q ratio is approximately constant over a range of GS adenylation states. Further data from Senior (Senior, 1975) indicate that at KG/Q ratios larger than 1.8, the adenylation state is less than 1, suggesting loss of robustness in the low regime of adenylation states. The present robust model (Equations 21–23, full line) agrees well with these measurements. Model parameters: Va/Vr = 1.8 KG/Q, maximal ternary to binary complex ratio 100:1, total GS/total AT = 100 (Chock et al., 1990).

These effects do not depend explicitly on the multimeric nature of GS, the substrate of the bifunctional enzyme. We find that AT/AR's bifunctional nature, coupled with GS being a multimer, can work together to provide a system level function: robustness of the ratio of α-ketoglutarate to glutamine in the face of wide variations in the levels of all of the proteins in the core circuit, and in the metabolic inputs such as ammonia and carbon source. The ratio is robust also to variations in the cell's demand for glutamine. This robustness means that the circuit can function properly to balance carbon and nitrogen fluxes despite the noise inherent in protein concentrations and the environment. The essence of the mechanism is based on avidity of the bifunctional enzyme AT/AR to adjacent monomers of GS on the same dodecamer.

To test this model, we used genetic perturbations, controlled gene expression, and mass spectrometry measurement of metabolite levels. We find that the ratio of glutamine to α-ketoglutarate is indeed robust to wide variations in the level of GS, and that this robustness depends on the bifunctional enzyme AT/AR. We further find that robustness carries through to the growth rate of the cells: growth rate is robust to wide variations in the levels of GS, and this robustness depends on AT/AR. Moreover, addition of a monofunctional AT/AR mutant in the presence of the native AT/AR enzyme abolishes robustness, in accordance with the model predictions.

RESULTS

Standard Models of the Nitrogen System Are Not Robust

We begin by describing a generic model for the core circuit in the nitrogen system. This core circuit includes the modification cycle of GS by AT/AR (abbreviated as AT) and the production and utilization of glutamine (abbreviated as Q). Like in previous models of this system (Goldbeter and Koshland, 1984; Mutalik et al., 2003; Stadtman and Chock, 1977), we do not include the multimeric nature of GS. As a result, varying the levels of the protein GS or the rates of Q utilization or synthesis in the model leads to proportionally large variations in the ratio of Q to KG. Thus, the model does not provide robustness.

Consider the following illustrative model: the production of Q occurs at rate proportional to the active (unadenylated) GS monomers, denoted GSo, and its utilization by the cell occurs at rate α Q (the utilization rate α is a function of conditions and growth rate), so that

$$dQ/dt = \beta\,GSo - \alpha\,Q. \quad (1)$$

Here, β describes the enzymatic velocity of GSo, which is a function of the availability of its substrates glutamate, ammonia, and ATP. At steady state, one finds that Q is proportional to GSo:

$$Qst = \beta/\alpha\,GSo. \quad (2)$$

The amount of GSo monomers is determined by the cycle of adenylation and deadenylation by AT/AR. Adenylation occurs when AT/AR binds GSo, in the complex [GSo AT], and removal of adenyl occurs similarly by the complex [GS_A AT]. At steady state, the concentration of these complexes is proportional to the product of their free constituent concentrations. One can thus describe this cycle given the effective rate constants for adenylation and deadenylation by AT/AR, denoted Va and Vr:

$$dGSo/dt = Vr\,AT\,GS_A - Va\,AT\,GSo. \quad (3)$$

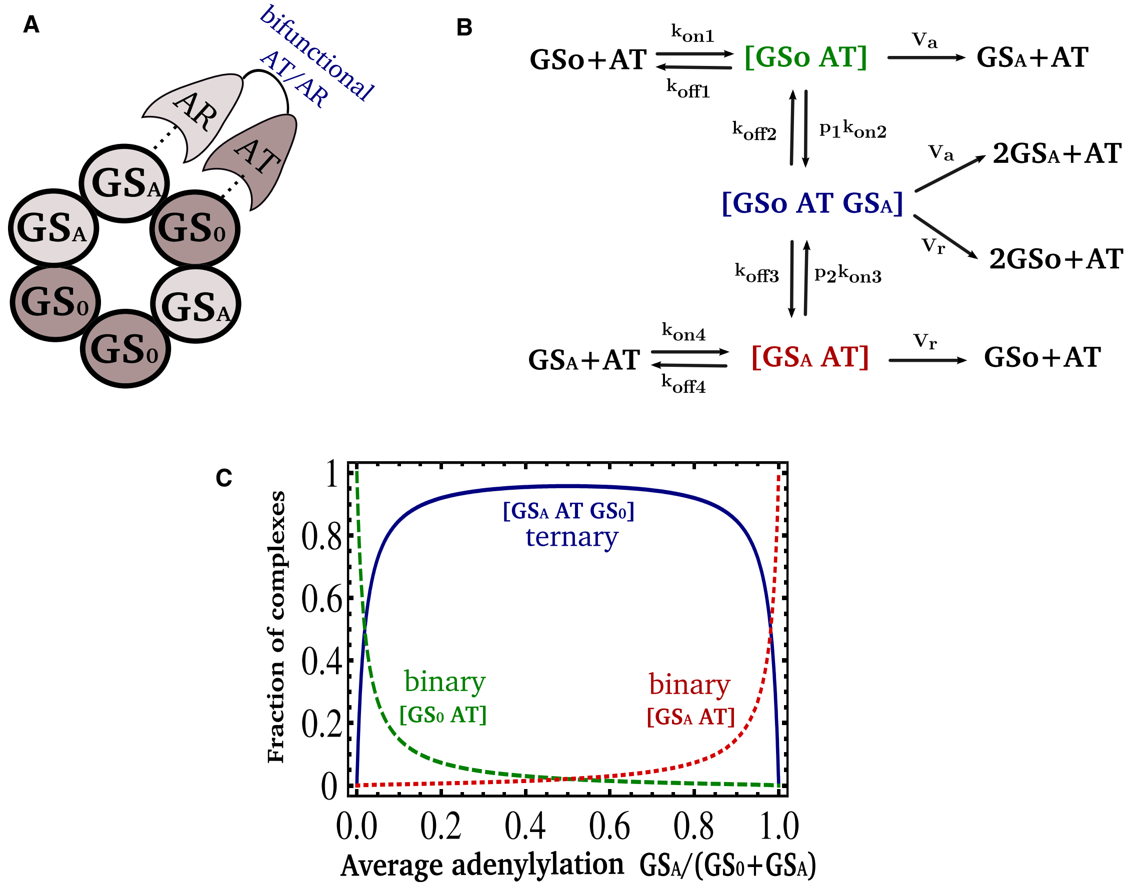

Figure 2. A Mechanism for Robustness Based on Avidity of the Two Domains of AT/AR to Two Adjacent Monomers in the GS Multimer

(A) Shown is an illustration of the ternary complex, in which the two domains of an AT/AR enzyme bind adjacent monomers of GS. The adenyl-transferase domain binds GSo, and the adenyl-removing domain binds GS_A. This double binding results in high avidity.

(B) Shown are reactions for the formation of binary and ternary complexes of AT/AR and GS. When one domain of AT/AR binds a monomer, the rate for binding an adjacent monomer by the second domain, Kon2 and Kon3, is very large.

(C) The fraction of AT/AR found in the ternary complex [GSo AT GS_A] is much higher than the fraction found in binary complexes with only one monomer [GS_A AT] or [GSo AT], over most of the range of GS adenylation levels. In this plot the parameters, normalized to Koff1 and total AT, are Kon1 = Kon4 = 0.01[Koff1/AT], Koff4 = Koff1, Kon2 = Kon3 = 100[Koff1], Koff2 = Koff3 = 1[Koff1], Va = Vr = 0.1[Koff1] and total GS/total AT = 100 as observed (Chock et al., 1990; Jiang et al., 2007a).

At steady state, one finds that GSo is proportional to the total amount of GS, $GS_T \approx GSo + GS_A$

$$GSo = Vr/(Va + Vr)GS_T. \quad (4)$$

Using this in Equation 2, one finds that Q at steady state depends on the total amount of GS, and also on the parameters α and β:

$$Qst = Vr/(Va + Vr)GS_T\ \beta/\alpha. \quad (5)$$

The amount of Q is thus dependent on the total levels of GS protein in the cell, and on the utilization and production rates α and β. This straightforward model is therefore not robust to either GS protein levels or fluctuations in the sources and sinks that affect α and β. Although a degree of insensitivity is conferred by the fact that Va and Vr depend on Q and KG, one cannot make Q/KG independent on protein levels or the parameters β and α. This is in line with models analyzed by metabolic control theory (Hofmeyr and Cornish-Bowden, 1991; Fell, 1996), in which variation in enzyme level or activity generally lead to direct variation in product. More detailed models including full mass-action kinetics, product inhibition, sublinear demand of glutamine, and a biphasic response to metabolite levels are likewise not robust (see section 5 in the Supplemental Information available online).

Mechanism for Robustness Based on Avidity of the Bifunctional Enzyme to GS Multimers

We now propose a mechanism, based on the biochemical details of the system, which can provide robustness. As above, glutamine is produced by GSo, as described in Equation 1. The mechanism differs from the one above in that it relies on the fact that GS is found in multimers (dodecamers) (Stadtman et al., 1970, 1980). It assumes that the two domains of the bifunctional AT/AR protein—the domains that add and remove the adenyl modification, respectively—can each bind adjacent monomers within this multimer (Figure 2A). Thus, AT/AR can bind GS either in a binary complex [GSo AT] and [GS_A AT], or in a ternary complex where it binds two GS monomers in the same multimer, [GSo AT GS_A]. The rate of GSo adenylation is therefore the sum of the contributions of the binary and ternary complexes with rates Vr and Va:

$$\begin{aligned} dGSo/dt = {} & Vr([GS_A\ AT] + [GSo\ AT\ GS_A]) \\ & - Va([GSo\ AT] + [GSo\ AT\ GS_A]). \end{aligned} \tag{6}$$

The fact that AT/AR has two domains, and its substrate is multimeric, allows for a strong cooperative effect in AT/AR binding, known as *avidity*. Binding of one AT/AR domain, say the adenyl-removing domain, to an adenylated monomer GS_A allows the second domain to bind an adjacent unadenylated monomer GSo. The binding of the second domain occurs very rapidly because of its high effective local concentration. As a result, the on-rate of the second binding event is much higher than the on-rate of the first binding event. Furthermore, unbinding of AT/AR now requires that both domains simultaneously unbind, which is a rare event. In this way, the avidity effect greatly increases the probability that both domains of AT/AR bind the same multimer of GS as compared to a situation where only one of the two domains binds.

The present avidity effect is analogous to the well-known avidity of multiheaded antibodies such as IgM to multivalent antigens (Crothers and Metzger, 1972; Karush, 1976). The present system is different from the case of antibodies in that the binding is of an enzyme to a substrate: the enzyme AT/AR can add/remove the modification of one of the two bound GS monomers, and then potentially dissociate.

As a result of avidity, the concentration of the ternary complex [GSo AT GS_A] is expected to be much higher than the concentration of the binary complexes. This is true as long as there are sufficient amounts of both types of monomers, GS_A and GSo (Figure 2C; a mathematical treatment of the avidity effect is presented in the Experimental Procedures). Reasonable parameter values for the present system indicate that the ternary complex is at least an order of magnitude more prevalent than the binary complexes, except when GSo or GS_A levels drop to less than 5% of the total GS amount.

When the ternary complex is so prevalent, one can, as a first approximation, neglect the contributions of the binary complexes in Equation 6. The ternary complex remains as the main catalyst of both adenyl addition and removal. Consider the system at steady state: the total rate of adenyl addition by the ternary complex equals that of removal,

$$Va(Q, KG)[GSo\ AT\ GS_A] = Vr(Q, KG)[GSo\ AT\ GS_A], \tag{7}$$

where the specific rates of adenyl addition Va and removal Vr, are regulated by glutamine (Q) and α-ketoglutarate (KG).

Importantly, the ternary complex cancels out from both sides of the equation, and thus steady state requires equality between the molecular rate constants

$$Va(Q, KG) = Vr(Q, KG). \tag{8}$$

The solution is that Q reaches a level relative to KG that satisfies this equation, and thus Q is a function of KG determined only by molecular rate constants

$$Q = f(KG). \tag{9}$$

Appropriate choice of the functional dependence of Va and Vr on the effectors KG and Q thus allows a constant ratio of Q and KG, as observed (Senior, 1975) (see the Experimental Procedures):

$$Q/KG = c^* = \text{const}. \tag{10}$$

Hence, the avidity mechanism can provide a steady-state Q/KG ratio that does not depend on any protein concentration. The Q/KG ratio also does not depend on the parameters α and β in Equation 1, which corresponds to the substrate-dependent velocity of GS and the utilization rate of Q by the cell. Thus, the Q/KG ratio is robust to protein levels and environmental fluctuations in ammonia and carbon availability. An analytical solution of the model shows that the robust Q/KG ratio is a stable fixed point of the dynamics (see section 13 in the Supplemental Information).

Intuitively, this mechanism works by placing both modification and demodification reactions into a single molecular species, the ternary complex. The multimeric nature of GS, together with the bifunctionality of AT/AR, gives rise to avidity that makes the ternary complex the most common type of complex. Fluctuations in the levels of this complex (originating from fluctuations in the levels of its constituent proteins) thus cancel out, because they strengthen both antagonistic reactions by the same amount. When production and degradation rates of Q vary, the system adjusts GS adenylation, and accordingly the rate of Q synthesis described by Equation 1, so that Q levels readjust until the robust ratio of Q and KG is restored. In summary, the avidity of AT/AR to multimeric GS can provide a robust Q/KG ratio: a ratio that is dependent only on molecular rate constants and does not depend on the levels of proteins in the cell or on the levels of nitrogen and carbon sources and sinks.

Robustness in the Present Mechanism Breaks Down in Extreme Nitrogen or Carbon Limitation, or When GS Levels Are Very Low

We next examined when robustness in the present mechanism is expected to break down. Solution of the avidity mechanism equations (Equations 1 and 6) shows that under severe nitrogen limitation the control system shifts to a nonrobust mode. In this regime, nearly all of the GS is unadenylated, GSo, and thus active. Q/KG ratios drop below the robust ratio c* (Figure 1B, low region of x axis).

The reason for this lack of robustness is that GS_A monomers become so rare that the ternary complex levels become comparable to binary complex levels, in which AT/AR binds only one monomer, [GSo AT]. This precludes the cancellation in Equation 7. The adenylation reaction is thus carried out mainly by a binary complex [GSo AT], whereas rare removals occur through the ternary complex [GSo AT GS_A], so that cancellation does not occur. Note that this breakdown of robustness is desirable, enabling a dropping Q/KG ratio to reliably signal nitrogen deprivation and trigger appropriate transcriptional responses. It is consistent with experimental data showing that glutamine levels fall during nitrogen limitation (Ikeda et al., 1996; Yuan et al., 2009; Brauer et al., 2006).

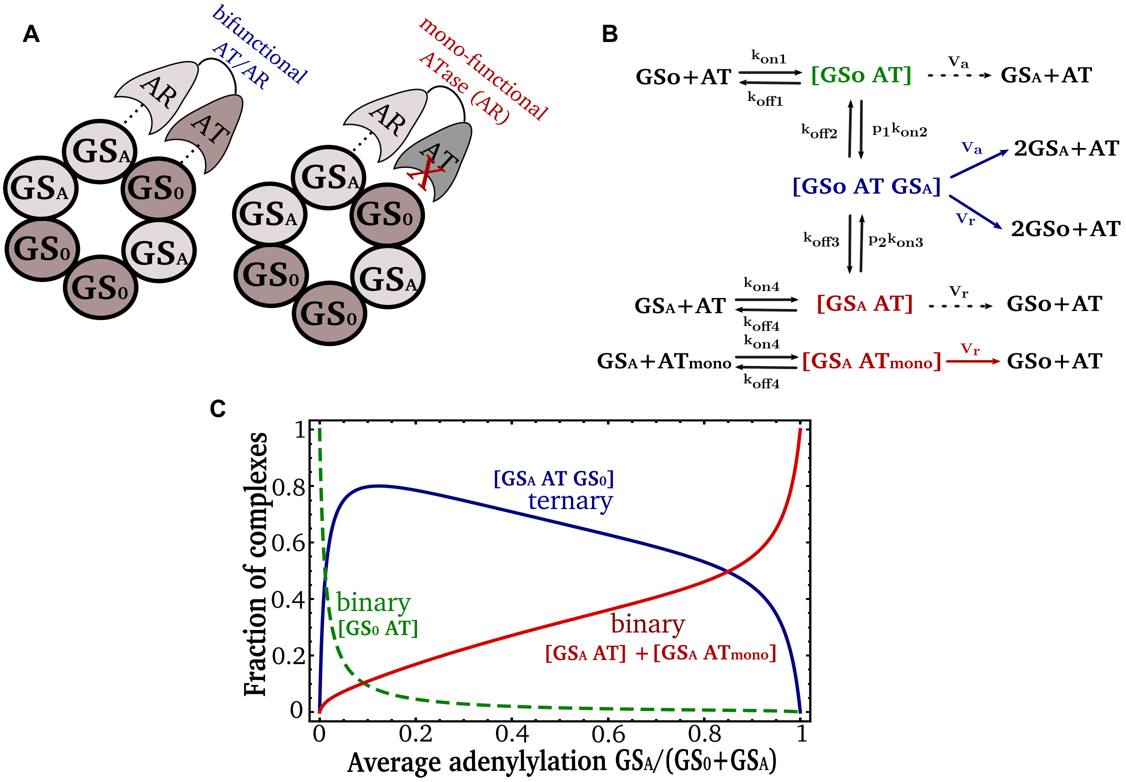

Figure 3. Addition of a Monofunctional AR Enzyme to the Native System Abolishes Robustness

(A) A schematic representation of the native AT/AR enzyme (AT) binding two adjacent monomers of GS (GSo and GS_A monomers) and a monofunctional version of AT/AR, AT_{mono}, that binds only GS_A to catalyze the adenyl-removal (AR) reaction.

(B) Reactions of the formation of binary and ternary complexes of AT/AR, AT_{mono}, and GS. While most reactions of AT/AR occur through the ternary complex, all reactions of the AT/AR mutant, AT_{mono}, occur through the binary complex [GS_A AT_{mono}], abolishing the robust ratio of glutamine to α-ketoglutarate.

(C) The fraction of AT/AR bound in the ternary complex is now comparable with the amount in the binary complex [GS_A AT_{mono}] over most of the range of GS adenylation levels. In this plot the parameters are as in Figure 2, and total AT_{mono}/total AT = 5.

Similarly, when nitrogen is plentiful but carbon is severely limiting, most GS monomers become adenylated, GS_A. In this way, the system nearly halts Q synthesis so as not to drain the depleted carbon pools of the cell (as mentioned above, Q synthesis draws KG from the TCA cycle, Figure 1A). Again the ternary complex is no longer prevalent, since GSo monomers are scarce, and Q/KG ratios become larger than the robust value (Figure 1B, high region of x axis). The mechanism thus shows non-robust modes at the extreme limits of GS adenylation or deadenylation, and robust behavior in intermediate adenylation levels. This agrees well with the observed Q/KG ratios under a variety of carbon-limited growth rates, as shown in Figure 1B (Senior, 1975).

A loss of robustness is also predicted to occur when GS protein levels are very low. In this case, the maximal possible GS activity cannot supply the required amounts of Q to maintain the Q/KG robust ratio. The ratio thus drops below its robust value.

In summary, a robust Q/KG ratio is expected throughout the range of conditions in which GS adenylation is neither close to zero nor complete, but rather at an intermediate level. An important physiological situation where robustness breaks down is during nitrogen limitation. In this case, a changing Q/KG ratio can act as a signal to trigger cellular adaptation to the low nitrogen environment (Ikeda et al., 1996; Yuan et al., 2009; Brauer et al., 2006).

Robustness in the Present Mechanism Is Expected to Break Down upon Introduction of a Monofunctional AT/AR Enzyme

The avidity mechanism also predicts that robustness breaks upon addition to the native system of a monofunctional version of the AT/AR enzyme that can bind only one type of GS subunits (either GS_A or GSo monomers). For example, consider a mutant enzyme that has only an adenyl-removing activity, and binds only GS_A (denoted AT_{mono}). Since it cannot bind two monomers at the same time, this mutant enzyme does not have the capacity for avidity. It catalyzes the removal reaction only from the binary complex [GS_A AT_{mono}]. The steady-state equation for the change in GS0 subunits now yields (compare with Equation 7)

$$\mathrm{Va(Q,KG)[GSo\ AT\ GS_A] = Vr(Q,KG)([GSo\ AT\ GS_A] + [GS_A\ AT_{mono}])}. \tag{11}$$

The cancellation of the ternary complex is now not possible, and the model predicts that the ratio between glutamine and α-ketoglutarate is no longer robust to GS levels or to metabolite levels (see Figure 3). Furthermore, the model predicts that loss of robustness is dependent on the ratio between the

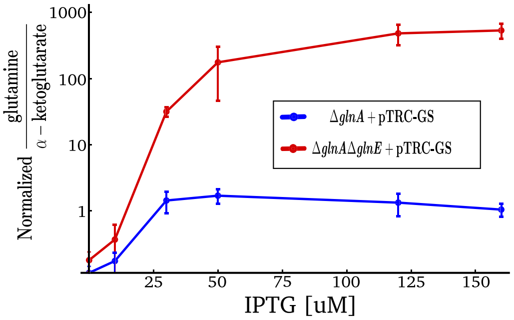

Figure 4. The Q/KG Ratio Is Robust to Variation in GS Protein Levels, and This Robustness Depends on AT/AR

In a strain deleted for the GS gene (*glnA*), and in which GS is expressed from an inducible plasmid, glutamine to α-ketoglutarate ratio varies by less than a factor of two above a threshold expression level (blue line). In a strain deleted for both the gene encoding AT/AR and the gene encoding GS, the glutamine to α-ketoglutarate ratio varies by over 500-fold for the same induction range. Both metabolite ratios were normalized to the corresponding ratio in a WT strain bearing a control vector induced with the same IPTG levels. Error bars are calculated from standard errors of metabolite measurements as defined in the Experimental Procedures section.

monofunctional and bifunctional AT/AR forms. The more AT_{mono} is expressed, the less robust the system becomes. Solution of Equation 11 and its implications are presented in the Supplemental Information, section 12. We now turn to experimental tests of the model.

The Q/KG Ratio Is Robust to GS Levels, and Robustness Depends on AT/AR

To test whether the Q/KG ratio is robust to variations in protein levels, we constructed *E. coli* strains in which GS level can be experimentally manipulated. For this purpose, we deleted the GS-encoding gene (*glnA*) from the chromosome and expressed GS from a plasmid under the control of an inducible *lac* promoter. Adding the inducer IPTG to these cells results in controlled variation in GS protein expression levels (Figure S8). Based on GFP expression from the same plasmid as well as RNA levels measurements (see section 8 in the Supplemental Information), we find that induction with IPTG spans about a 50-fold range of GS levels.

We measured the intracellular concentrations of Q, KG, and glutamate (E) in bacteria growing in glycerol minimal medium with ample nitrogen by means of liquid chromatography-tandem mass spectrometry (Rabinowitz, 2007; Brauer et al., 2006; Lu et al., 2008; Bennett et al., 2008). We compared these metabolite levels in the GS-induced strain to those of the parental wild-type strain (see Figure S1), at various IPTG levels. We find that across the full range of GS induction levels the ratio Q/KG varies by less than a factor of 2 (Figure 4, blue line).

We repeated this experiment in a strain deleted also for the AT/AR-encoding gene, *glnE*. In this strain, we find that the Q/KG ratio is not robust to GS induction. The Q/KG ratio varies over 500-fold as GS is induced by IPTG (Figure 4, red line). This indicates that robustness of the Q/KG ratio depends on the bifunctional enzyme AT/AR.

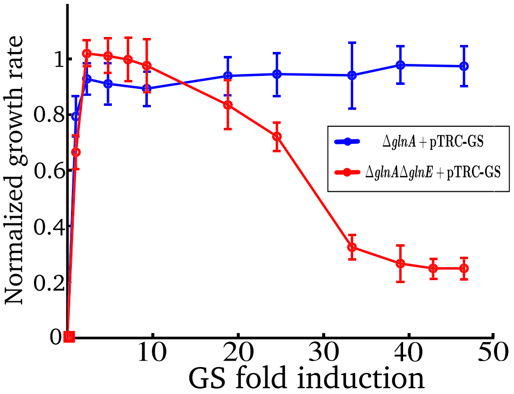

Figure 5. Growth Rate Is Robust to GS Levels, and This Robustness Depends on AT/AR

In a strain deleted for *glnA*, and in which GS is expressed from an inducible plasmid, growth rate is insensitive to variations in GS above a threshold minimal expression level (blue line). In a strain deleted for both the AT/AR and GS genes (*ΔglnA ΔglnE*), the growth rate is no longer robust to GS induction, falling with increasing GS expression (red line). The zero induction point (square) corresponds to the deletion strains without the GS expression plasmid. Growth rate is normalized to the growth rate of wild-type strain in the same conditions bearing a control vector. Fold induction was calculated with respect to uninduced GS expression (0 μM IPTG, see the Supplemental Information). Error bars are standard deviations.

Growth Rate Is Robust to GS Levels, and Robustness Depends on AT/AR

We next asked, does the robustness in the GS circuit carry through to the growth rate of the cells? If so, one can expect that growth rate will be robust to changes in the total GS protein level, and that this robustness will depend on the presence of AT/AR. One might also expect that under conditions where robustness is predicted to break down (such as very low levels of GS, or severe nitrogen limitation), robustness of growth rate to GS levels will likewise be lost.

In order to test the robustness of the growth rate, we measured the exponential growth rate of the cells as a function of GS induction levels, in a glycerol minimal medium with ample nitrogen. We compared this to the growth rate of the parental wild-type strain bearing a control vector. Growth rate was measured using a robotic system in 96-well plates, over two generations of exponential growth, at a day-to-day accuracy of about 1% as described (Dekel and Alon, 2005).

We find that growth rate is robust to wide variations in GS enzyme levels, and is similar to that of the wild-type strain (Figure 5, blue line). Growth rate declines only when GS expression is low.

We repeated this experiment in the strain deleted for AT/AR (*glnE*). We find that the growth rate increases sharply with GS levels, reaches a maximum close to the wild-type growth rate, and then declines when GS expression is further increased (Figure 5, red line). In the absence of AT/AR, rapid growth is thus found only in a restricted range of GS induction levels. Similar results are found when we used another carbon source (acetate), displaying an even narrower range of high growth rates (Figure S3C). Similar narrow range of induction levels for high growth was also found in a strain expressing a monofunctional enzyme capable of only adenyl-removal activity (denoted AT-CDN, see Figure S3A), in the absence of native AT/AR.

These results agree with experiments by Kustu and colleagues (Kustu et al., 1984), who measured growth rate of several *S. typhimurium* strains which were deleted for AT/AR (*glnE*) and expressed aberrant levels of GS (by mutations in the *glnA* promoter). These studies indicated that in the absence of AT/AR, a low and a high expression level of GS reduces the cell's growth rate.

Growth rate was found to be also robust to variations in AT/AR levels. We tested the effect of varying AT/AR expression on growth rate by constructing a strain deleted for both AT/AR (*glnE*) and GS (*glnA*) where both enzymes levels are controlled exogenously by inducible plasmids. AT/AR was expressed under a *lac* promoter, and GS was expressed under a *tet* promoter. GS was expressed at high levels using saturating levels of the inducer aTc, and AT/AR was varied using increasing levels of IPTG. We find that in this strain, growth rate is robust to wide variations in the levels of AT/AR (Figure S2).

Robustness Is Abolished by Coexpression of a Monofunctional AT/AR Mutant in the Presence of the Native AT/AR Enzyme

The results shown so far indicate that the nitrogen system is robust to variation in the levels of its core enzymes and that this robustness depends, as predicted by the model, on AT/AR.

In order to further test the avidity mechanism, we introduced a monofunctional AT/AR mutant enzyme to the native system. The model predicts that in case of a combined expression of wild-type AT/AR enzyme together with a monofunctional enzyme that is unable to form a ternary complex with GS, robustness will be lost (see above, it should be noted that in case of expression of a monofunctional enzyme which can form a ternary complex, the model predicts that robustness will be partially preserved with respect to GS levels).

To test this hypothesis, we constructed a strain in which the GS gene (*glnA*) is deleted from the chromosome. This strain has an intact AT/AR gene (*glnE*). GS expression was controlled with IPTG as described above. In addition, a mutant AT/AR gene encoding for a monofunctional enzyme with only AR activity (bearing the mutations D701N and D703N, designated AT-CDN; Jiang et al., 2007b) was expressed from a plasmid under a *tet* promoter. This strain expresses both the native AT/AR enzyme and the monofunctional AT-CDN enzyme capable of catalyzing only adenyl-removal reactions. We measured growth rate of this strain at different GS induction levels in acetate minimal medium with ample nitrogen. In this experiment, acetate—a relatively poor carbon source—was used in order to place carbon limitation on the cells, so that excess GS activity that draws KG from the TCA cycle causes a more marked effect on growth rate than in better carbon sources (glycerol, glucose).

We find that when AT-CDN is not induced (in the absence of the *tet* promoter inducer aTc), growth rate is robust with respect to varying GS levels (Figure 6, blue line). Upon expression of AT-CDN (5 nM aTc), we find that growth rate depends on GS total levels (Figure 6, red line), and thus robustness is abolished.

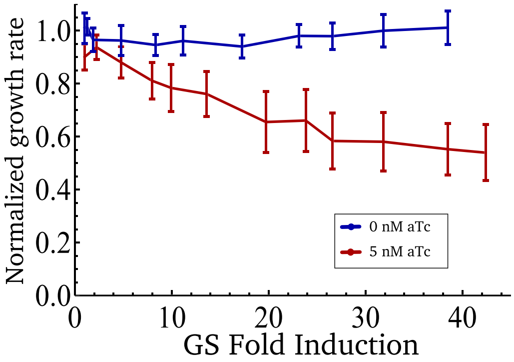

Figure 6. Addition of a Monofunctional Mutant AT/AR Enzyme to the Native System Abolishes Robustness

In a strain deleted for *glnA*, and in which GS is expressed from an inducible plasmid while the monofunctional enzyme is not induced from its plasmid (0 nM aTc), growth rate is robust to variations in GS (blue line). In the same strain induced by 5 nM aTc to express the monofunctional mutant of AT/AR (AT-CDN), growth rate depends on GS expression levels. Growth rate was normalized to the growth rate of a strain expressing an intact AT/AR enzyme (*glnE*) from the same plasmid at the same levels of IPTG and aTc. Error bars are standard deviations.

Loss of robustness is not observed in a control strain that is identical except that it expresses wild-type AT/AR under the *tet* promoter, instead of AT-CDN.

We find that growth rates become more sensitive to variations in GS levels the higher the expression of the monofunctional enzyme AT-CDN (Figure S3B). This corresponds to the model predictions that in the present strain the Q/KG ratio depends on the ratio between monofunctional to bifunctional enzyme levels (see section 12 in the Supplemental Information).

Transcriptional Upregulation of the GS-Encoding Gene Occurs Only under Severe Nitrogen Limitation

We further tested the dependence of growth rate on GS levels in severe nitrogen limitation. We find that under nitrogen-limiting conditions (1% of the NH_4 in the M9 minimal medium formula) growth rate increases with GS (Figure S4A) and is therefore not robust to GS levels. This is in line with the predictions of the breakdown of robustness in the model in severe nitrogen limitation.

Finally, we asked how the transcriptional control of the GS-encoding gene, *glnA*, can be understood in the context of the robust features of the system. In conditions in which the system is robust to protein levels, it does not make sense to regulate the expression of its proteins. Only when robustness to protein levels breaks down can transcriptional control be useful to change the state of the cell (Miyashiro and Goulian, 2008).

We therefore studied the transcriptional activity of the *glnA* promoter by means of a GFP reporter strain (Zaslaver et al., 2006). In minimal glucose medium with ample nitrogen, we find that the *glnA* promoter shows a constant low activity throughout exponential growth that declines upon entry into stationary phase. In contrast, in a medium with low nitrogen (1% of the NH_4 in the minimal medium formula), we find that the *glnA* promoter activity increases sharply for about one generation upon entry into stationary phase (Figure S4B), consistent with experiments by Ninfa and colleagues (Atkinson et al., 2002;

Blauwkamp and Ninfa, 2002). This suggests that a significant increase in *glnA* transcription occurs only as nitrogen becomes sharply limiting. These results concur with the current picture, where the system is robust to GS levels when nitrogen is ample, and that robustness breaks down at limiting nitrogen, requiring increased transcription to provide elevated GS activity.

DISCUSSION

The present study presents a model showing that the nitrogen assimilation circuit of *E. coli* can maintain a robust ratio between the metabolites Q and KG in the face of wide variation in protein levels and fluctuations of metabolite sources and sinks. This robustness is based on a combination of bifunctionality and avidity: the bifunctional modifying enzyme AT/AR can show avidity by binding simultaneously to two monomers within a GS multimer. We found using mass spectrometry and accurate growth measurements that the Q/KG ratio, as well as the cells' growth rate, is robust to controlled variations in GS levels, and that this robustness depends on the bifunctional enzyme AT/AR. The addition of a monofunctional version of AT/AR to the system abolishes robustness, as predicted by the model. The present experiments are also consistent with the known conditions in which robustness of the Q/KG ratio breaks down, such as extreme nitrogen limitation.

The present experiments suggest that growth rate is robust to GS levels across at least a 50-fold range of expression. This range might be relevant physiologically, especially upon transition from nitrogen-limiting conditions (in which GS is very highly expressed) to carbon-limiting conditions. Without robustness, such a shift would cause excess GS to draw too much KG from the TCA cycle, draining the carbon resources of the cell, and impairing growth. Robustness ensures that the system is able to seamlessly adjust to large changes in conditions.

The proposed avidity mechanism allows for optimal balance between two primary growth-limiting factors, nitrogen and carbon. In times of carbon shortage, the mechanism finely tunes the rate of nitrogen assimilation to avoid draining KG from the TCA cycle. It would be interesting to see if similar mechanisms operate at other important branch points in metabolism, to balance between conflicting needs of systems sharing the same precursor.

It is interesting to relate the present robust mechanism to other known mechanisms for robustness of biological circuits with respect to variations in protein levels (reviewed in Tyson et al., 2003; Barkai and Shilo, 2007; Kitano, 2004; Alon, 2007). A number of metabolic fluxes have been shown experimentally to be insensitive to variations in enzyme levels (Kacser and Burns, 1973; LaPorte et al., 1985), a central finding in the context of metabolic control analysis (Fell, 1996). Detailed molecular mechanisms for this robustness are not known. Specific mechanisms for robustness have also been studied in nonmetabolic systems. Robust adaptation has been well-characterized in bacterial chemotaxis (Alon et al., 1999; Barkai and Leibler, 1997; Yi et al., 2000), as have robust patterning and scaling in morphogenesis (Eldar et al., 2002; Ben-Zvi et al., 2008).

More recently, bifunctional enzymes have been suggested to allow robust input-output relationships in bacterial signaling (Batchelor and Goulian, 2003; Shinar et al., 2007) and of flux in the glyoxylate bypass (Shinar et al., 2009). The present avidity mechanism provides a new example of a robust control circuit that relies on a bifunctional enzyme that catalyzes two opposing reactions. It is thus related to the mechanisms in bacterial signaling and glyoxylate systems. However, the nitrogen mechanism also has key biochemical differences from these systems. In particular, the nitrogen mechanism relies on avidity of the bifunctional enzyme to two substrate monomers within a multimer, a feature that is lacking in the other mechanisms. This avidity feature is crucial in making the ratio of Q and KG, rather than the flux of Q production, the robust feature of the model.

The relation between robustness to protein levels and transcriptional control was also explored. We find that *glnA* transcription becomes highly active only when nitrogen is severely limiting. At this severe limitation, the AT/AR control loop is at its limit, with all GS unadenylated and active. Transcription can allow increased uptake of nitrogen, boosting GS activity by raising its protein levels. A related feature was observed by Goulian et al. in the *phoQphoP* two-component system, where transcriptional control (positive autoregulation) of this robust system is functionally important mainly at the outer range of the system performance (Miyashiro and Goulian, 2008). Note that transcriptional control acts on the timescale of minutes, whereas the modification control by AT/AR acts in seconds to allow response to rapid variations.

It would be of interest to directly test the avidity effect in vitro—perhaps by assaying whether the fraction of adenylated GS monomers affects the specific rate of adenylation and deadenylation by the bifunctional enzyme. Moreover, the present model was tested using a monofunctional AT-CDN version of AT/AR, expressed in parallel to the native system. The model predicts loss of robustness in the case that AT-CDN cannot form a tertiary complex with its substrate, and only a partial loss if it can. The present data support the former interpretation. It would be of interest to further test directly the ability of AT-CDN to bind to its substrate with its nonfunctional C-terminal subunit.

It is likely that robust mechanisms also operate in other systems with bifunctional enzymes with multimeric substrates. For example, in C4 plants the bifunctional enzyme PPDK acts on a multimeric substrate (Chastain and Chollet, 2003). Such robust mechanisms might enable precise control of key metabolite levels.

The present approach can be used to theoretically and experimentally test the robustness in other key metabolic circuits that control growth. It provides a context for the bifunctionality of AT/AR and the multimeric structure of its substrate GS, suggesting that biochemical details that might seem arbitrary on their own can work together to provide robustness. It furthermore provides an initial example of the potential for geometrical organization of enzymes to contribute to the overall robustness of metabolism.

EXPERIMENTAL PROCEDURES

Strains and Plasmids

A list of strains and plasmids used in this work is provided in Table S6. A detailed description of strains construction is provided in the Supplemental Information, sections 6 and 7.

Growth Conditions and Measurements

Robustness of growth rate to changes in GS, AT/AR, and monofunctional AT-CDN levels was explored by accurate measurements of the average growth rate in a robotic system in a 96-well plate format, using different induction levels of the proteins of interest, expressed from IPTG- or aTc-inducible plasmids (pTrc99 and pZA31, respectively, see Table S6). Error bars in Figures 5 and 6 are standard deviation of 48 wells per induction level.

We used three carbon sources in order to apply varying degrees of carbon limitation to the cells: glucose for high carbon, glycerol for intermediate carbon, and acetate for low carbon. Glycerol (0.4%) was used as the main carbon source. Sodium acetate (0.25%) was used as a poor carbon source in the experiments where the monofunctional AT-CDN enzyme was expressed in the presence of the native AT/AR enzyme. For nitrogen-limiting conditions, the same assay was used with M9 containing 1% (185 μM) of the NH_4 in the regular formula and 0.2% glucose instead of glycerol.

Range of Controlled Expression

The range of controlled expression from the pTrc plasmid under the present experimental conditions was measured by two assays: (1) expressing GFP from the same plasmid and measuring fluorescence at different induction levels, and (2) quantitative RT-PCR of GS mRNA at different induction levels (see the Supplemental Information). Based on data such as Figure 5 to find the induction level that gives growth rates comparable to the wild-type strain, we estimate that the range of GS expression is from 0.3 ± 0.1 to about 16 ± 4 times wild-type levels.

Culture Conditions and Metabolite Extraction for Mass Spectrometry

Detailed protocols for preparing filter cultures and extracting metabolites have been published (Yuan et al., 2008). In brief, filter cultures were prepared by passing 5 ml of exponentially growing liquid batch culture through membrane filters. The filters were then placed on top of agarose loaded with the appropriate minimal media. All strains were cultured in minimal salts media (Gutnick et al., 1969) with 10 mM NH_4Cl and 0.4% glucose at 37°C, unless otherwise noted. Plates contained, in addition to the appropriate media, 1.5% ultrapure agarose (triply washed with cartridge-filtered water to remove trace organic contaminants). Control experiments showed that this medium gives essentially the same growth rate robustness results as M9-based media.

To quench metabolism and initiate extraction, the filters were submerged directly into −20°C 40:40:20 acetonitrile:methanol:water with 0.1% formic acid. The cells extracts were collected and mixed with isotope-labeled internal standard compounds (the ten listed in Bajad et al., 2006, as well as isotope-labeled glutamine) and stored at 4°C until analysis.

Metabolite Measurement

Cell extracts were analyzed, within 24 hr of their preparation, by LC-electrospray ionization (ESI)-MS on a Thermo Exactive Orbitrap mass spectrometer, using a modified version of the ion-pairing reversed phase chromatography reported in Lu et al. (2008). For individual metabolites, all data presented are average ± SEM of three biological replicates. For Q/KG plotted in Figure 4, the following equations were used to calculate the value and error:

$$(Q/KG)_{MT}/(Q/KG)_{WT} = (Qavg/KGavg)_{MT}/(Qavg/KGavg)_{WT} \tag{12}$$

$$\delta R_{\frac{MT}{WT}} = R_{\frac{MT}{WT}} \times \sqrt{\left(\frac{\delta R_{MT}}{R_{MT}}\right)^2 + \left(\frac{\delta R_{WT}}{R_{WT}}\right)^2}, R = \frac{Q_{Avg}}{KG_{Avg}} \tag{13}$$

where MT and WT stand for mutant strain and wild-type, Q_{avg} represents the average signal of glutamine in the strain specified, and KG_{avg} represents the average signal of α-ketoglutarate in the strain specified. The error of Q/KG for each strain (the δR = δ[Qavg/KGavg] terms) were calculated as following

$$\delta R = \delta\left(\frac{Q_{avg}}{KG_{avg}}\right) = \left(\frac{Q_{avg}}{KG_{avg}}\right) \times \sqrt{\left(\frac{\delta Q_{avg}}{Q_{avg}}\right)^2 + \left(\frac{\delta KG_{avg}}{KG_{avg}}\right)^2}. \tag{14}$$

Mathematical Model for Ternary Complex Avidity

We use mass-action kinetics to describe the model illustrated in Figure 2B:

$$\begin{aligned} d[\text{GSo AT}]/dt = {} & \text{Kon1 GSo AT} - (\text{Koff1} + \text{Va} + \text{Kon2 p1})[\text{GSo AT}] \\ & + \text{Koff2}[\text{GSo AT GS}_A] = 0 \end{aligned} \tag{15}$$

$$\begin{aligned} d[\text{GS}_A\ \text{AT}]/dt = {} & \text{Kon4 GS}_A\ \text{AT} - (\text{Koff4} + \text{Vr} + \text{Kon3 p2})[\text{GS}_A\ \text{AT}] \\ & + \text{Koff3}[\text{GSo AT GS}_A] = 0 \end{aligned} \tag{16}$$

$$\begin{aligned} d[\text{GSo AT GS}_A]/dt = {} & \text{Kon2 p1}[\text{GSo AT}] + \text{Kon3 p2}[\text{GS}_A\ \text{AT}] \\ & - (\text{Koff2} + \text{Koff3} + \text{Va} + \text{Vr})[\text{GSo AT GS}_A] = 0. \end{aligned} \tag{17}$$

Here p1 denotes the probability for a GS_A monomer near a bound GSo monomer, and p2 is the same for a GSo monomer near a bound GS_A monomer. The simplest model assumes that p1 and p2 are the fractions of the corresponding monomers

$$\text{p1} = \text{GS}_A/\text{GS}_T \tag{18}$$

$$\text{p2} = \text{GSo}/\text{GS}_T. \tag{19}$$

A more detailed model that takes into account the spatial configurations of GSo and GS_A in the dodecamer is provided in the Supplemental Information. This model shows similar results for robustness and makes further predictions on the correlations of the states of adjacent monomers.

These equations were solved analytically under the assumption that GS concentration is much higher than AT/AR levels (about a 100-fold excess of GS over AT/AR occurs in this system [Chock et al., 1990]). The avidity effect makes the on-rates for AT/AR already bound to one monomer to bind an adjacent monomer on the same dodecamer very large, due to the increased local concentration (Kon2,Kon3 $\gg$ Kon1 GS_T, Kon4 GS_T). Also, off-rates are assumed to be much faster than enzymatic reactions rates, as is the case for most enzymes (in vitro experiments show Va,Vr in the range of 1–10 [1/s] (Jiang et al., 2007a), whereas typical Koff values are on the order of 1000/s given that the enzymes Km is on the order of 1 μM. Thus Va,Vr $\ll$ Koff1,Koff4). Analytical solution of the model was obtained using Mathematica 6.0. A lower bound for the ratio of ternary to binary complexes is (see the Supplemental Information for details)

$$[\text{GSo AT GS}_A]/([\text{GS}_A\ \text{AT}] + [\text{GSo AT}]) \approx \text{A}\ \min(\text{p1}, \text{p2}) \gg 1 \tag{20}$$

where A ≈ Kon2/Koff2 is estimated to be on the order of 100 (Crothers and Metzger, 1972). The prevalence of the ternary complex breaks down only when the probabilities p1 or p2 become small, on the order of 1/A.

Mathematical Model for Robust Mechanism

To describe the adenylylation state as a function of the ratio between metabolite levels (see Figure 1B), we used the following model:

$$\begin{aligned} & \text{Va}(Q, KG)([\text{GSo AT}] + [\text{GSo AT GS}_A]) \\ & \quad - \text{Vr}(Q, KG)([\text{GS}_A\ \text{AT}] + [\text{GSo AT GS}_A]) = 0 \end{aligned} \tag{21}$$

$$\beta[\text{GSo}] - \alpha\, Q = 0 \tag{22}$$

$$\text{Va}(Q, KG)/\text{Vr}(Q, KG) = 1.8\ Q/KG \tag{23}$$

where Va and Vr are effective adenylation and deadenylation rates, [GSo AT] and [GS_A AT] are the concentrations of the binary complexes, and [GSo AT GS_A] is the ternary complex concentration. β is the synthesis rate of glutamine which is a function of substrate availability, and α is the utilization rate of glutamine. Equation 23 represents the ratio between the rates of the antagonistic reactions catalyzed by AT/AR. For example, if the rates follow Michaelis-Menten-like forms for the two effectors Q and KG, so that Va = V_{a0} Q/Z, Vr = V_{r0} KG/Z, and Z = 1 + Q/K_Q + KG/K_{KG}, one can obtain Va/Vr = V_{a0}/V_{r0} Q/KG. For Figure 1B (full line), complex concentrations were used from the avidity model described in the previous section (Equations 15–17) where the maximal fraction of ternary complex equals to 0.95 (see Figure 2C). These equations were solved numerically using Mathematica 6.0 where the parameter on the curve was $\lambda = \alpha/\beta$. λ is the equivalent of the growth rate parameter in Senior's measurements (Senior, 1975).

SUPPLEMENTAL INFORMATION

Supplemental Information includes 11 figures, Supplemental Experimental Procedures, and Supplemental References and can be found with this article at doi:10.1016/j.molcel.2010.12.023.

ACKNOWLEDGMENTS

We thank H. Mori and the National BioResource Project (NIG, Japan) for the Keio collection. We thank A.J. Ninfa and P. Jiang for the AT-CDN plasmid. We thank N. Barkai, R. Milo, T. Tlusty, and G. Shinar for helpful discussions and insightful comments. This work was supported by the Israel Science Foundation, the Kahn Family Foundation, and the European Research Council.

Received: March 2, 2010
Revised: August 5, 2010
Accepted: November 24, 2010
Published: January 6, 2011

REFERENCES

Alon, U. (2007). An Introduction to Systems Biology: Design Principles of Biological Circuits (New York: CRC Press).

Alon, U., Surette, M.G., Barkai, N., and Leibler, S. (1999). Robustness in bacterial chemotaxis. Nature *397*, 168–171.

Atkinson, M.R., Blauwkamp, T.A., Bondarenko, V., Studitsky, V., and Ninfa, A.J. (2002). Activation of the glnA, glnK, and nac promoters as Escherichia coli undergoes the transition from nitrogen excess growth to nitrogen starvation. J. Bacteriol. *184*, 5358–5363.

Bajad, S.U., Lu, W., Kimball, E.H., Yuan, J., Peterson, C., and Rabinowitz, J.D. (2006). Separation and quantitation of water soluble cellular metabolites by hydrophilic interaction chromatography-tandem mass spectrometry. J. Chromatogr. A *1125*, 76–88.

Barkai, N., and Leibler, S. (1997). Robustness in simple biochemical networks. Nature *387*, 913–917.

Barkai, N., and Shilo, B. (2007). Variability and robustness in biomolecular systems. Mol. Cell *28*, 755–760.

Batchelor, E., and Goulian, M. (2003). Robustness and the cycle of phosphorylation and dephosphorylation in a two-component regulatory system. Proc. Natl. Acad. Sci. USA *100*, 691–696.

Bennett, B.D., Yuan, J., Kimball, E.H., and Rabinowitz, J.D. (2008). Absolute quantitation of intracellular metabolite concentrations by an isotope ratio-based approach. Nat. Protoc. *3*, 1299–1311.

Ben-Zvi, D., Shilo, B.Z., Fainsod, A., and Barkai, N. (2008). Scaling of the BMP activation gradient in Xenopus embryos. Nature *453*, 1205–1211.

Blauwkamp, T.A., and Ninfa, A.J. (2002). Physiological role of the GlnK signal transduction protein of *Escherichia coli*: survival of nitrogen starvation. Mol. Microbiol. *46*, 203–214.

Brauer, M.J., Yuan, J., Bennett, B.D., Lu, W., Kimball, E., Botstein, D., and Rabinowitz, J.D. (2006). Conservation of the metabolomic response to starvation across two divergent microbes. Proc. Natl. Acad. Sci. USA *103*, 19302–19307.

Chastain, C.J., and Chollet, R. (2003). Regulation of pyruvate, orthophosphate dikinase by ADP-/Pi-dependent reversible phosphorylation in C3 and C4 plants. Plant Physiol. Biochem. *41*, 523–532.

Chock, P.B., Rhee, S.G., and Stadtman, E.R. (1990). Metabolic control by the cyclic cascade mechanism: a study of E. coli glutamine synthetase. In Control of Metabolic Processes, A. Cornish-Bowden, A. Cardenas, and M.L. Cardenas, eds. (New York: Plenum Press), pp. 183–194.

Crothers, D.M., and Metzger, H. (1972). The influence of polyvalency on the binding properties of antibodies. Immunochemistry *9*, 341–357.

Dekel, E., and Alon, U. (2005). Optimality and evolutionary tuning of the expression level of a protein. Nature *436*, 588–592.

Eldar, A., Dorfman, R., Weiss, D., Ashe, H., Shilo, B.Z., and Barkai, N. (2002). Robustness of the BMP morphogen gradient in Drosophila embryonic patterning. Nature *419*, 304–308.

Fell, D. (1996). Understanding the Control of Metabolism, First Edition (Burlington, VT: Ashgate Publishing).

Goldbeter, A., and Koshland, D. (1984). Ultrasensitivity in biochemical systems controlled by covalent modification. Interplay between zero-order and multistep effects. J. Biol. Chem. *259*, 14441–14447.

Gutnick, D., Calvo, J.M., Klopotowski, T., and Ames, B.N. (1969). Compounds which serve as the sole source of carbon or nitrogen for Salmonella typhimurium LT-2. J. Bacteriol. *100*, 215–219.

Hofmeyr, J.S., and Cornish-Bowden, A. (1991). Quantitative assessment of regulation in metabolic systems. Eur. J. Biochem. *200*, 223–236.

Ikeda, T.P., Shauger, A.E., and Kustu, S. (1996). Salmonella typhimurium apparently perceives external nitrogen limitation as internal glutamine limitation. J. Mol. Biol. *259*, 589–607.

Jaggi, R., van Heeswijk, W.C., Westerhoff, H.V., Ollis, D.L., and Vasudevan, S.G. (1997). The two opposing activities of adenylyl transferase reside in distinct homologous domains, with intramolecular signal transduction. EMBO J. *16*, 5562–5571.

Jiang, P., Peliska, J.A., and Ninfa, A.J. (1998). The regulation of Escherichia coli glutamine synthetase revisited: role of 2-ketoglutarate in the regulation of glutamine synthetase adenylylation state. Biochemistry *37*, 12802–12810.

Jiang, P., Mayo, A.E., and Ninfa, A.J. (2007a). Escherichia coli glutamine synthetase adenylyltransferase (ATase, EC 2.7.7.49): kinetic characterization of regulation by PII, PII-UMP, glutamine, and alpha-ketoglutarate. Biochemistry *46*, 4133–4146.

Jiang, P., Pioszak, A.A., and Ninfa, A.J. (2007b). Structure-function analysis of glutamine synthetase adenylyltransferase (ATase, EC 2.7.7.49) of Escherichia coli. Biochemistry *46*, 4117–4132.

Kacser, H., and Burns, J.A. (1973). The control of flux. Symp. Soc. Exp. Biol. *27*, 65–104.

Kamberov, E.S., Atkinson, M.R., and Ninfa, A.J. (1995). The Escherichia coli PII signal transduction protein is activated upon binding 2-ketoglutarate and ATP. J. Biol. Chem. *270*, 17797–17807.

Karush, F. (1976). Multivalent binding and functional affinity. Contemp. Top. Mol. Immunol. *5*, 217–228.

Kitano, H. (2004). Biological robustness. Nat. Rev. Genet. *5*, 826–837.

Kustu, S., Hirschman, J., Burton, D., Jelesko, J., and Meeks, J.C. (1984). Covalent modification of bacterial glutamine synthetase: physiological significance. Mol. Gen. Genet. *197*, 309–317.

LaPorte, D.C., Thorsness, P.E., and Koshland, D.E. (1985). Compensatory phosphorylation of isocitrate dehydrogenase. A mechanism for adaptation to the intracellular environment. J. Biol. Chem. *260*, 10563–10568.

Lu, W., Bennett, B.D., and Rabinowitz, J.D. (2008). Analytical strategies for LC-MS-based targeted metabolomics. J. Chromatogr. B Analyt. Technol. Biomed. Life Sci. *871*, 236–242.

Miyashiro, T., and Goulian, M. (2008). High stimulus unmasks positive feedback in an autoregulated bacterial signaling circuit. Proc. Natl. Acad. Sci. USA *105*, 17457–17462.

Mutalik, V.K., Shah, P., and Venkatesh, K.V. (2003). Allosteric interactions and bifunctionality make the response of glutamine synthetase cascade system of Escherichia coli robust and ultrasensitive. J. Biol. Chem. *278*, 26327–26332.

Neidhardt, F.C., and Curtiss, R. (1996). Escherichia Coli and Salmonella/Cellular and Molecular Biology, Second Edition (Washington, DC: ASM Press).

Ninfa, A.J., and Atkinson, M.R. (2000). PII signal transduction proteins. Trends Microbiol. *8*, 172–179.

Rabinowitz, J.D. (2007). Cellular metabolomics of Escherchia coli. Expert Rev. Proteomics *4*, 187–198.

Rhee, S.G., Chock, P.B., and Stadtman, E.R. (1989). Regulation of Escherichia coli glutamine synthetase. Adv. Enzymol. Relat. Areas Mol. Biol. *62*, 37–92.

Senior, P.J. (1975). Regulation of nitrogen metabolism in Escherichia coli and Klebsiella aerogenes: studies with the continuous-culture technique. J. Bacteriol. *123*, 407–418.

Shapiro, B.M., and Stadtman, E.R. (1970). The regulation of glutamine synthesis in microorganisms. Annu. Rev. Microbiol. *24*, 501–524.

Shinar, G., Milo, R., Martínez, M.R., and Alon, U. (2007). Input output robustness in simple bacterial signaling systems. Proc. Natl. Acad. Sci. USA *104*, 19931–19935.

Shinar, G., Rabinowitz, J.D., and Alon, U. (2009). Robustness in glyoxylate bypass regulation. PLoS Comput. Biol. *5*. 10.1371/journal.pcbi.1000297.

Stadtman, E.R., and Chock, P.B. (1977). Superiority of interconvertible enzyme cascades in metabolic regulation: analysis of monocyclic systems. Proc. Natl. Acad. Sci. USA *74*, 2761–2765.

Stadtman, E.R., Ginsburg, A., Ciardi, J.E., Yeh, J., Hennig, S.B., and Shapiro, B.M. (1970). Multiple molecular forms of glutamine synthetase produced by enzyme catalyzed adenylation and deadenylylation reactions. Adv. Enzyme Regul. *8*, 99–118.

Stadtman, E.R., Hohman, R.J., Davis, J.N., Wittenberger, M., Chock, P.B., and Rhee, S.G. (1980). Subunit interaction of adenylylated glutamine synthetase. Mol. Biol. Biochem. Biophys. *32*, 144–156.

Tyson, J.J., Chen, K.C., and Novak, B. (2003). Sniffers, buzzers, toggles and blinkers: dynamics of regulatory and signaling pathways in the cell. Curr. Opin. Cell Biol. *15*, 221–231.

Yi, T.M., Huang, Y., Simon, M.I., and Doyle, J. (2000). Robust perfect adaptation in bacterial chemotaxis through integral feedback control. Proc. Natl. Acad. Sci. USA *97*, 4649–4653.

Yuan, J., Bennett, B.D., and Rabinowitz, J.D. (2008). Kinetic flux profiling for quantitation of cellular metabolic fluxes. Nat. Protoc. *3*, 1328–1340.

Yuan, J., Doucette, C.D., Fowler, W.U., Feng, X.J., Piazza, M., Rabitz, H.A., Wingreen, N.S., and Rabinowitz, J.D. (2009). Metabolomics-driven quantitative analysis of ammonia assimilation in E. coli. Mol. Syst. Biol. *5*. Published online August 18, 2009. 10.1038/msb.2009.60.

Zaslaver, A., Bren, A., Ronen, M., Itzkovitz, S., Kikoin, I., Shavit, S., Liebermeister, W., Surette, M.G., and Alon, U. (2006). A comprehensive library of fluorescent transcriptional reporters for Escherichia coli. Nat. Methods *3*, 623–628.